

Computational Modalities of Belousov-Zhabotinsky Encapsulated Vesicles

Julian Holley, Andrew Adamatzky, Larry Bull, Ben De Lacy Costello,
Ishrat Jahan

Abstract

We present both simulated and partial empirical evidence for the computational utility of many connected vesicle analogs of an encapsulated non-linear chemical processing medium. By connecting small vesicles containing a solution of sub-excitable Belousov-Zhabotinsky (BZ) reaction, sustained and propagating wave fragments are modulated by both spatial geometry, network connectivity and their interaction with other waves. The processing ability is demonstrated through the creation of simple Boolean logic gates and then by the combination of those gates to create more complex circuits.

Keywords: Belousov-Zhabotinsky reaction, computation, logic gates, half adder, excitable media, unconventional computing

1. Introduction

The last half of the twentieth century has been witness to huge leaps in technology spanning all areas of science. One of the most noticeable areas has been the dramatic success of the vonn Neumann [41] architecture electronic digital computer. Although modern digital computers or the software has not advanced to a point where one computer could independently create another technologically superior computer, or where software could compose more advanced software¹, one could argue that from a purely technological perspective such a point has already been passed. It is has now become extremely difficult to design future computers (and develop their software)

¹A so called point of singularity.

without the aid of existing computers (and software development tools). In spite of such advances the current computer architecture will always struggle with certain problems.² Attempting to advance computing beyond the current dogma, lays the field of ‘*Unconventional Computing*’ [6]. This is an area of study that explores alternative computational representation, substrates and strategies, the results of which not only create novel experimental processing devices [1], but also contribute towards algorithms operating on conventional serial digital computers. One direction in this genre is the study of reaction diffusion (RD) computing [4]. Where the innate behaviour of a chemical reaction and subsequent diffusion in space and time can be used to present and manipulate information. A suitable and convenient chemical reaction for such processing is the Belousov-Zhabotinsky (BZ) reaction, a type of reaction that is subject to non-equilibrium thermodynamics creating a nonlinear chemical oscillator [44]. In certain formulations the BZ reaction can produce visible travelling waves which can be used to represent information [43]. Wave development is effected not only by the reaction conditions, but by geometric obstacles and collisions with other waves. Computation *circuits* analogous to electronic circuits can be created with chemical pathways (conductors) routed through a passive substrate (insulator) with waves representative of signals (electron flow).

In order to illustrate the possibility of computation in a BZ substrate some of the key components that are used to create electronic digital computers have been created, such as; diodes [10, 15, 22], coincidence detector [19] and logic gates [38, 35, 26, 18]. These components have been combined to create more complex circuits such as memory [27, 17, 16], counters [19] and binary adders [9]. These circuits serve to demonstrate that it is possible to create computational devices by modelling existing digital components and functions within the RD frame work, this approach amounts to conventional computing on an unconventional substrate. More interesting are some systems that exemplify unconventional processing and media, such as robot control [7, 2] shortest path calculation [36, 32, 33, 11, 3], image processing [24, 8], information encoding [13] and direction detection [28].

Contrary to these previous computation approaches in a BZ medium we have focused on exploring the utility of connecting small spherical process-

²For example problems known to be NP hard, where the scale of the problem is known, the solution easily tested, but a solution remains intractable with current algorithms.

ing elements containing BZ medium (vesicles) into functional networks [29]. Vesicles can be created by surrounding a solution of BZ reactant with a monolayer of lipids [34]. This cell like structure has some interesting parallels with real neurons. When two or more vesicles are pressed together in solution the gap between the lipid layer forms a chemical junction similar to a synaptic cleft. Transmission of excitation from one vesicle to another could be possible and the effectiveness modulated by the suspension solution. Furthermore the oscillatory nature of the BZ reaction can be likened to the up-state firing (excitation) and down-state (inhibition) of neural activity. Travelling waves can be created when the BZ solution is in a sub excitable mode and waves can be used to represent information signals, analogous to electrical spike trains in neurons. Connections between vesicles could be arranged in such a way as to create functional nuclei (Fig. 1). Reaction transmission in mono-layer lipid coated droplets (2D vesicles) of oscillating BZ solution has recently been reported [37].

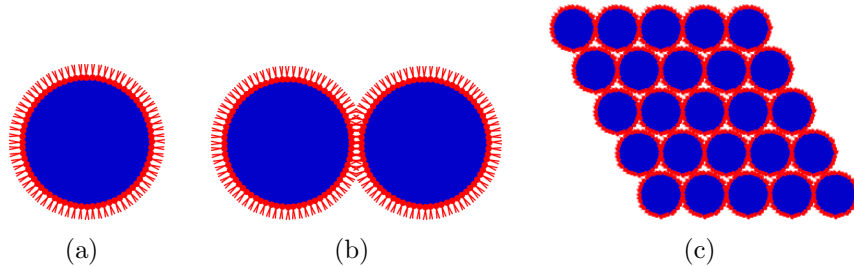


Figure 1: (a) Lipid coated mono-layer (red) vesicle enclosing BZ solution (blue). (b) Two vesicle lipid monolayers link to form a lipid bi-layer membrane connection. (c) Hexagonal array of lipid linked vesicles.

In terms of connection, self adaptation and longevity the vesicle~neuron analogy does not hold. Real neurons are typified by their distributed connectedness, ability to learn and self sustain. Vesicles under consideration in this work are only connected locally, also they cannot be sustained beyond exhaustion of the reagent and at this point no adaptation mechanism has been devised. Nevertheless the rich phenomenological behaviour of the BZ reaction connected in complex networks could give rise to functions and insight to the sort of processing achieved by biological circuits.

The remainder of the paper is comprised of the following: Section 2.1 details the method of BZ numerical computer simulation and graphical presentation. Section 2.2 introduces vesicle simplification, geometry and net-

working. Simulation results exploring the vesicle geometry, connectivity and membrane function are presented in section 2.3. Elementary logic gates are presented in section 3.1 and more complex circuits are presented in section 3.2 & 3.3. The results are discussed, future directions considered and a summary presented in the remaining sections 4, 5 & 6.

2. Methods

2.1. Computer simulations

We have employed a two variable version of the Oregonator model [30] as a model of the BZ reaction [43, 44] adapted for photo-sensitive modulation of the Ru-catalysed reaction [23].

$$\begin{aligned}\frac{\partial u}{\partial t} &= \frac{1}{\epsilon}(u - u^2 - (fv + \phi)\frac{u - q}{u + q}) + D_u \nabla^2 u \\ \frac{\partial v}{\partial t} &= u - v\end{aligned}$$

Variables u and v are the local instantaneous dimensionless concentrations of the bromous acid autocatalyst activator HBrO_2 and the oxidised form of the catalyst inhibitor $\text{Ru}(\text{bpy})_3^{3+}$. ϕ symbolises the rate of bromide production proportional to applied light intensity. Bromide Br^- is an inhibitor of the Ru-catalysed reaction, therefore excitation can be modulated by light intensity; high intensity light inhibits the reaction. Dependant on the rate constant and reagent concentration ϵ represents the ratio of the time scales of the two variables u and v . q is a scaling factor dependent on the reaction rates alone. The diffusion coefficients D_u and D_v of u and v were set to unity and zero respectively. The coefficient D_v is set to zero because it is assumed that the diffusion of the catalyst is limited.

Numerical simulations were achieved by integrating the equations using the Euler-ADI³ method [31] with a time step $\delta t = 0.001$ and a spatial step $\delta = 0.25$. Experimental parameters are given in Tab. 1.

Networks of discs were created by mapping 2 different ϕ values (proportional to light intensity) onto a rectangle of homogeneous simulation substrate. To improve simulation performance the rectangle size was automatically adapted depending on the size of the network, but the simulation point

³Alternating direction implicit method.

Parameter	Value	Description
ϵ	0.022	Ratio of time scale for variables u and v
q	0.0002	Propagation scaling factor
f	1.4	Stoichiometric coefficient
ϕ	\star	Excitability level (proportional to light level)
u	\sim	Activator HBrO_2
v	\sim	Inhibitor $\text{Ru}(\text{bpy})_3^{3+}$
D_u	1.0	Activator diffusion coefficient
D_v	0	Inhibitor diffusion coefficient
Δx	0.25	Spatial step
Δt	0.001	Time step

Table 1: Kinetic and numerical values used in numerical simulations of (Eq. 1). $\star \phi$ Varies between two levels, sub-excited ($L1$) and inhibited ($L2$), $\phi_{L1} = 0.076$, $\phi_{L2} = 0.209$

density remained constant throughout. The excitation levels, $L1 \rightarrow L2$ relate to the partially active disc interiors and non-active substrate.

Discs are always separated by a single simulation point wide boundary layer. Connection apertures between discs are created by superimposing another small *link* disc at the point of connection (typically a $2 \rightarrow 6$ simulation point radius), simulation points have a 1:1 mapping with on screen pixels. The reagent concentrations are represented by a red and blue colour mapping; the activator, u is proportional to red level and inhibitor, v proportional to blue. The colour graduation is automatically calibrated to minimum and maximum levels of concentration over the simulation matrix. The background illumination is mono-chromatically calibrated in the same fashion proportional to ϕ , white areas are inhibitory and dark areas excited.

Wave fragment flow is represented by a series of superimposed time lapse images (unless stated otherwise), the time lapse is 50 simulation steps. To improve clarity, only the activator (u) wave front progression is recorded. Figure 2 illustrates the same wave fragment in both colour map (u & v) and time lapse versions (u).

Inputs are created by perturbing a small circular area of the activator (u) set to a value of 1 with a radius of 2 simulation points in the center of the disc. All discs representing inputs and outputs are highlighted with a blue and green border respectively.

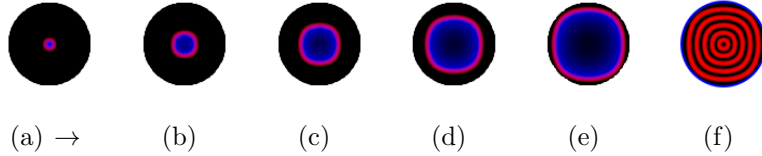


Figure 2: Example the time lapse image creation. The image shown in (f) is the accumulation of successive images shown from central wave initiation in (a) to extinction in (e). Time lapses periods are 50 time steps and the refractory tail of the inhibitor (u) shown in blue is not shown in the time lapse image to improve clarity. The outer blue boundary indicates an input disc when placed in a network.

2.2. Vesicle geometry, connectivity and networking

The three dimensional (3D) vesicle connection opportunities and complex internal wave reactions represent a rich computation substrate. Such depth raises difficulties when attempting to manually explore computation modalities. To reduce the complexity to a level where manual design is tractable the vesicles in this study have been approximated into two dimensional (2D) vesicles (discs). A disc is created by extracting an imaginary central slice, a cross section of a BZ vesicle (Fig. 3). This reduction also permits the opportunity of easily reproducing simulations by projecting circuits onto a 2D photo sensitive BZ gel. Signals are discrete, wave fragments represent the presence or absence of a particular signal.

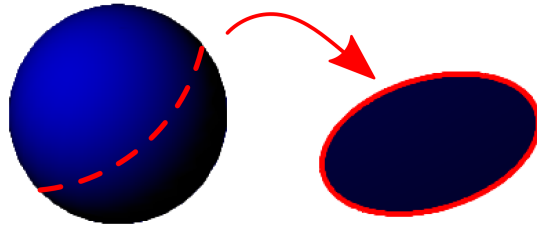


Figure 3: BZ vesicle to BZ disc. A 2D cross section of 3D vesicle of sub-excitable BZ medium is selected to create a *BZ disc*. A general purpose unit of connectivity and computation investigated during these initial explorations.

In a previous study we have shown that logic circuits can be created with uniform discs arranged in hexagonal networks [9], hexagonal packing

being the most efficient method of sphere (disc) packing. Further opportunities to modulate wave fragment behaviour are presented when disc size, connection angle and connection efficacy are combined in non-homogeneous networks. Disc size can be adjusted to permit or restrict internal wave interactions, producing either larger reaction vessel discs or smaller communications discs (Fig. 4a). Connection angle between discs can be used to direct wave collisions (Fig. 4b) and connection efficiency can effect the wave focus (Fig. 4c).

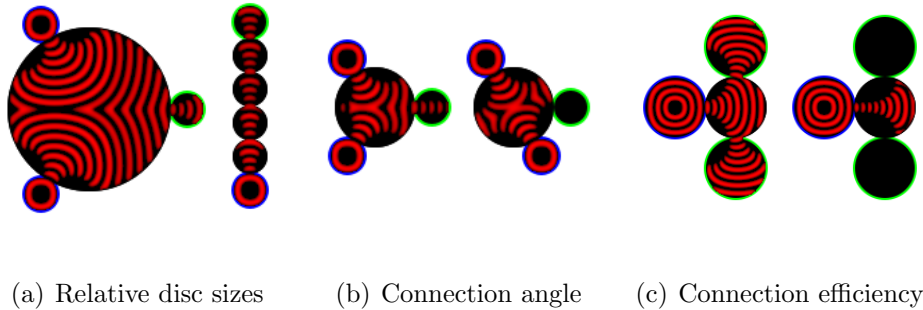


Figure 4: (a) Discs as reaction vessels in the left network or communication channels in the right network. (b) The effect of connection angle, the two input signals combine in the left network to produce an output. Adjusting the angle of the lower input in the right network alters the result of the collision and no output is produced. (c) The effect of connection efficiency. Large aperture (6 points) connection in the left network results in a broad spreading beam. Conversely a smaller (4 point) aperture connection in the right network creates a narrow beam wave. (In all images, inputs occur in discs circled in blue, outputs circled in green.)

2.3. Computer simulation experiments

Increasing the relative disk size can be used not only to allow space for wave fragment collisions (Fig. 4a) but other effects are also apparent. Figure 5 illustrates the front development of the same wave through progressively smaller terminating discs. In the larger discs the wave fragment has more space in which to develop and spreads out to the majority of the disc perimeter, conversely in the smaller discs the wave fragment doesn't have time to develop and terminates almost directly opposite the entry aperture.

Wave fragments cannot survive when the fragment mass drops below some critical level [25] and this is evident when comparing progressively smaller

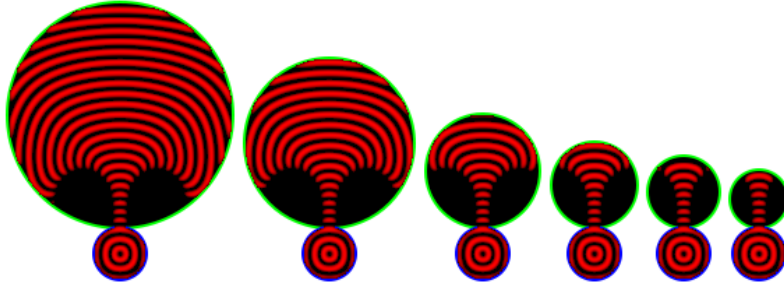


Figure 5: Wave fragment propagating from an fixed lower input disc of size 18 units to variable upper larger discs of radius 80 (left), 60, 40, 30, 25 & 20 (right) units. Source disc has a radius of 18 points and a connection aperture of 4 units.

aperture sizes with fixed size discs. In our system and with a disc radius of 28 units⁴ the critical level surrounds an aperture gap of 4 units. Below that fragments do propagate through the aperture but quickly die. The narrow beam produced as a result of a 4 unit aperture (type J1) presents an opportunity to deflect the wave to alternate exits and perform ballistic style computation [14]. We have found that using a narrow beam aperture in orthogonal networks where wave fragments do not normally propagate into connected perpendicular discs particularly useful in creating simple logic gates (Sect. 3.1). Furthermore, diode junctions can be created when networks of narrow (type J1) and broadband (type J2) are combined (Sect.3.2). Although more functionality could be achieved with more subtle aperture adjustments [5] further explorations in this work rely on combining just the two types, narrow (J1) and broadband (J2) (Fig. 4c).

3. Results

3.1. Elementary logic gates

Electronic logical gates form the building blocks of more complex digital circuitry forming the foundations of complex high level components such as microprocessors. Although we do not envisage creating traditional vonn Neumann architecture microprocessors in BZ vesicles, the ability to create simple logic gates with BZ vesicles demonstrates that (like electronics) the

⁴Simulation grid points.

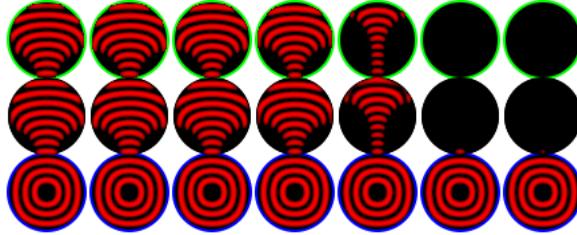


Figure 6: Comparison of aperture sizes. All disc sizes remain fixed at 28 units whilst the aperture is reduced from 8 (leftmost) to 2 units (rightmost).

medium and architecture is *capable* of such processing. Logic gates and composite circuits of logic gates have been created several times before using the BZ substrate, for example [38, 35, 26, 18]. Here we illustrate a selection of key gates can be created using nothing other than interconnected BZ discs. Figure 7 illustrates the operation of the most elementary of gates the inverter (NOT gate). The circuit operation starts with the simultaneous application of the circuit input (left most disc) in conjunction with the source (permanent logical ‘1’) input (top most disc). The circuit operation terminates by observing the output disc (lower most disc) at a time when either result state would be present. If the progression of a wave fragment through a disc is considered as 1 step then the output disc will hold a valid result after 2 steps from the application of the source input. Incorporating a parallel unmodulated source signal that travels from output to input could also be used to indicate the point at which the output discs holds a valid output. In this case this would simply consist of 3 serial discs.

The operation of an AND gate and the inversion, the NAND gate are shown in Fig. 8 & Fig. 9. The result of a wave collision in the NOT gate was exploited to deflect and extinguish the source wave into the disc edge, whereas in the AND gate the collision between the two inputs results in 2 perpendicular fragments, one of which develops in the output cell to produce the result.

A NAND gate can be created by combining the NOT gate and the AND gate Fig.9. NAND gates are known as *universal* gates since all other gates can be created from arrangements of NAND gates alone.⁵ The NOT gate

⁵NOR gates are also universal gates.

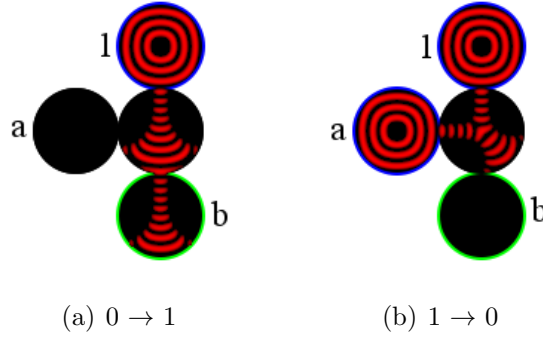


Figure 7: Inverter gate ($a = \bar{b}$) where the input (a) is center left (blue ring), bottom disc (green ring) is the output (b) and a supply, or source logical '1' top most disc (blue ring). (a) $a = 0$ The gate initiates with the source pulse in the top disc. In this case, no signal is present at the input disc and the source pulse travels to the output disc (bottom) resulting in a logical 1 output ($1 \rightarrow 0$). (b) $a = 1$ Again the source pulse travels from top to bottom, but in this case a collision with a signal present on the input disc produces a logical 0 output. ($0 \rightarrow 1$).

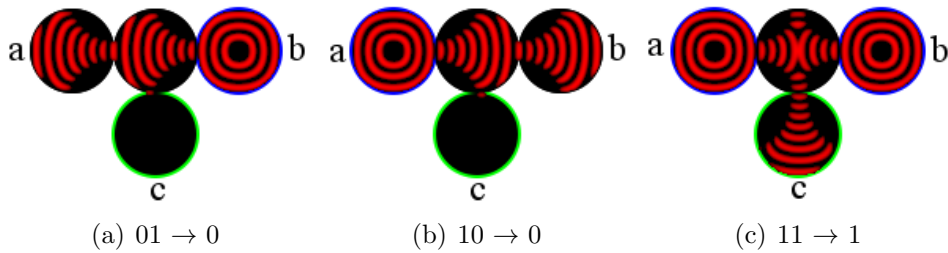


Figure 8: Two input AND gate ($c = a \bullet b$) where inputs a, b are top left and right discs (blue rings) and output c is the bottom central disc (green ring). (a) $(a, b)(0, 1)$ A wave from input b propagates uninterrupted and terminates in the opposing input disc a . (b) $(a, b)(1, 0)$ Likewise, a wave from input b propagates uninterrupted and terminates in the input disc b . (c) $(a, b)(1, 1)$ Waves from both input discs a and b collide in the central disc and eject two perpendicular waves, one of which propagates into the output disc (c).

(Fig. 7) is integrated below the AND gate in the lower row (Fig. 8) where the activity of a horizontal source signal inverts the vertical output.

The OR gate is used to detect the presence of one or more signals. A logical '1' on any input results in an output (Fig. 10). Common amongst all these gates, the output value of a logical '1' or '0' as indicated by the presence or absence of wave is only valid at a specific point in the development and

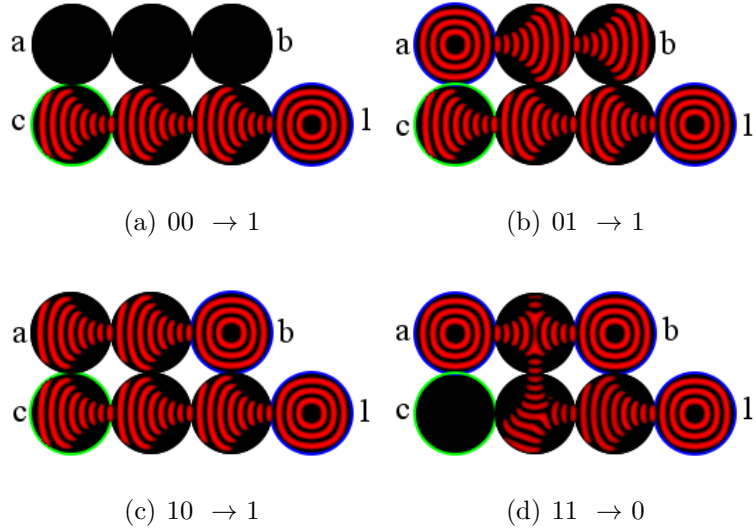


Figure 9: Two input NAND gate ($c = \overline{a \bullet b}$) where inputs a, b are top left and right discs (blue rings) and output c is the bottom left disc (green ring), source input is located on the bottom right (blue ring). Operation is identical to the AND gate (Fig. 8) but with an inverter (Fig. 7) integrated along the bottom disc row. (a), (b) & (c) The source input provides a logical '1' output for all input combinations other than $(a, b)(1, 1)$. (d) $(a, b)(1, 1)$ Output from the AND gate portion of the gate collides with the source input creating a logical '0' output.

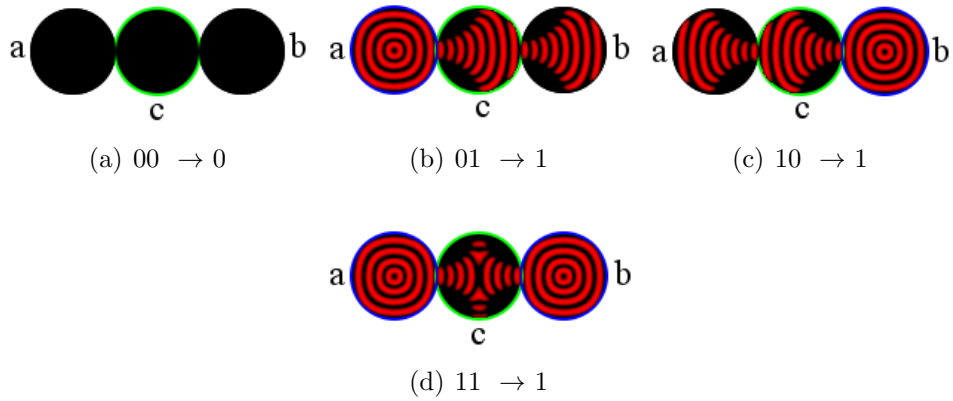


Figure 10: Two input OR gate ($c = a + b$) where inputs a, b are left and right discs (blue rings) and the central disc is the output c (green ring).

in these instances, approximated to be proportional to time. For example the OR gate output is sampled after a wave fragment has travelled by one disc unit ($t_d = 1$). Therefore the annihilation of the $(a, b)(1, 1)$ case and the continuation of the waves into opposing input cells for cases $(a, b)(0, 1)$ and $(a, b)(1, 0)$ does not effect the outcome.

The XOR gate is used to signal a difference between signals, producing an output when inputs alternate regardless of the composition of the difference. Figure 12 illustrates the BZ disc implementation along with the inversion NXOR in Fig. 11.

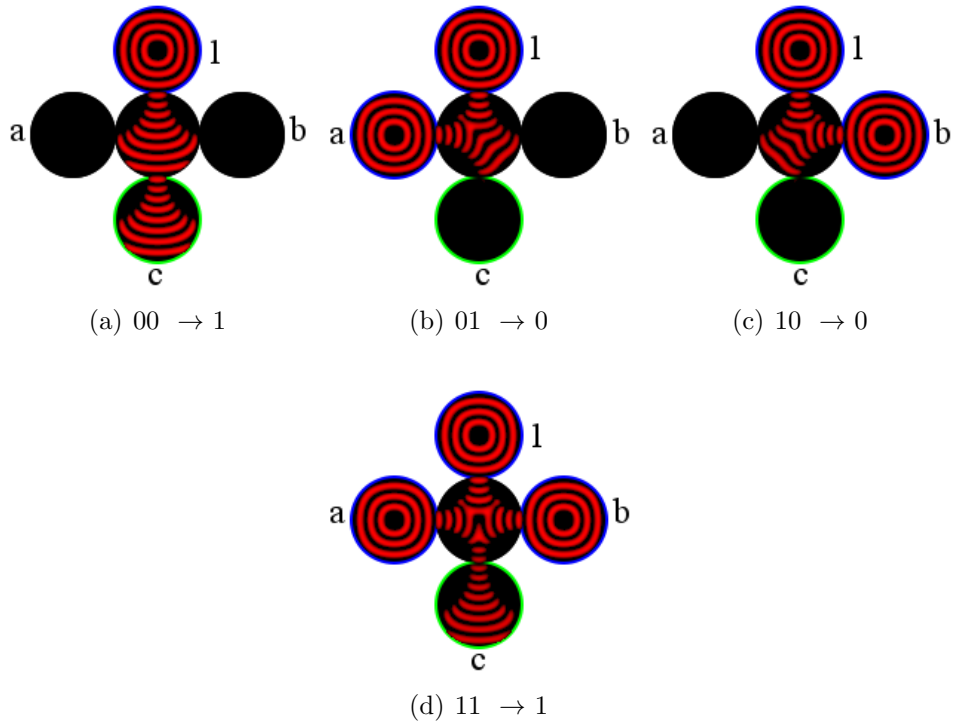


Figure 11: Two input NXOR gate ($c = \overline{a \oplus b}$) where inputs are middle row left and right (blue rings), the output disc is center bottom (green ring) and source input center top (blue ring). The OR structure (Fig 10) is repeated in the central row, the output of which deflects the source input from the center top disc, the result is an NXOR gate. The output of the NXOR can then be inverted to create a XOR gate (Fig. 12).

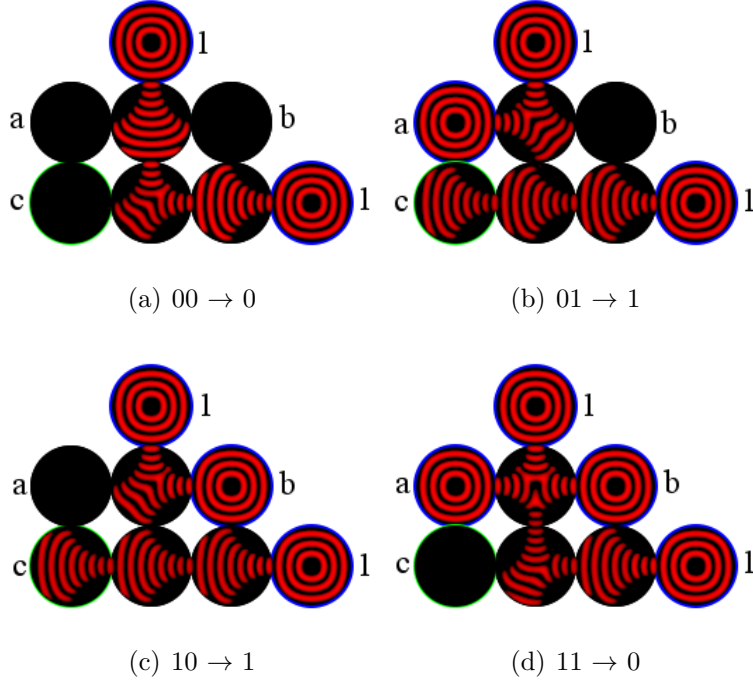


Figure 12: Two input XOR gate ($c = a \oplus b$) where inputs are middle row left and right (blue rings), the output disc is bottom left (green ring) and there are two source inputs, center top and bottom right (blue rings). The gate is an extension of the inverting the NXOR gate (Fig. 11).

3.2. Half adder

The half adder is a sub-system used in binary addition circuits. The half adder adds two binary digits and when connected with another half adder creates a full 1 bit adder. One bit adders can then in turn be connected together to make n^{th} bit adders (Fig. 13). A half adder can be constructed from a combination of two logic gates the XOR and AND gate. There are two inputs (a & b) and two outputs (S & C), the binary sum (S) of a & b is achieved by the XOR gate ($S = a \oplus b$) and inability of the configuration (overflow) to present the $1 + 1$ input is achieved with a carry (C) output, ($C = a \bullet b$).

A 1 bit half adder created from BZ discs can also be constructed from connecting a BZ disc AND gate and XOR gate (Sect. 3.1). Figure 14 shows the BZ disc conjunction for the half adder circuit. The input a needs to

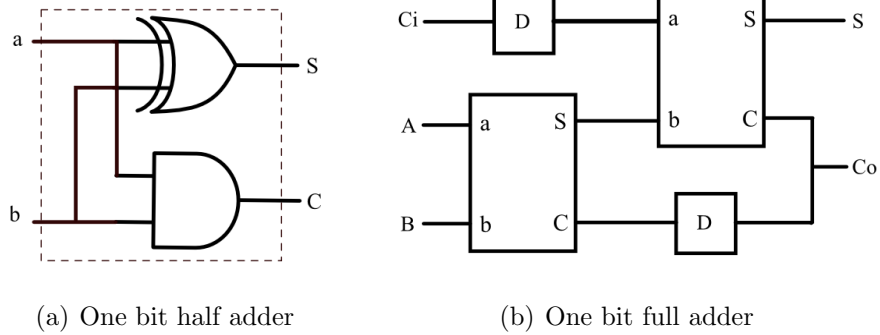


Figure 13: (a) One bit half adder. The circuit comprises of two outputs, the sum (S) derived from the XOR gate ($S = a \oplus b$) and carry (C) derived from the AND gate ($C = a \bullet b$). (b) One bit full adder. Two half adders can be cascaded together to create a full 1 bit adder ($S = C_i \oplus (a \oplus b)$, $C_o = a \bullet b + (a \oplus b)$). In turn full 1 bit adders can be cascaded to create an N bit adder. The D blocks represent signal delays required in order to synchronise signal pulses from different sources.

be repeated on the other side of input b in order for this circuit to work. This is necessary in order to overcome the *signal passing problem*, a universal problem for systems where signals propagate along specific planular channels. There are two ways to overcome this problem, either add identity to the signals in such a way that signals can share the medium or share the medium at different times. How two or more waves could be identified and share the same space in this BZ system remains unclear because of the diffusive nature of the reaction. However sharing a channel medium in time⁶ is possible if the time difference between signals is large enough to prevent the refractory tail from one extinguishing the other. Figure 15 illustrates one such temporal separation strategy, where signal a passes over signal b but becomes shifted in time. The circuit operates with two types of apertures, one that creates a narrow beam (type J1) wave and another that creates a broad beam (type J2) wave. Signals a & b travel from bottom to top, with a on the left and b on the right. The signal a is split at the junction to the first disc and a fragment a' travels horizontally towards b . Meanwhile b is already traversing the first disc and has progressed into the final disc before a' crosses the b

⁶In communications systems this is known as Time Division Multiplexing (TDM).

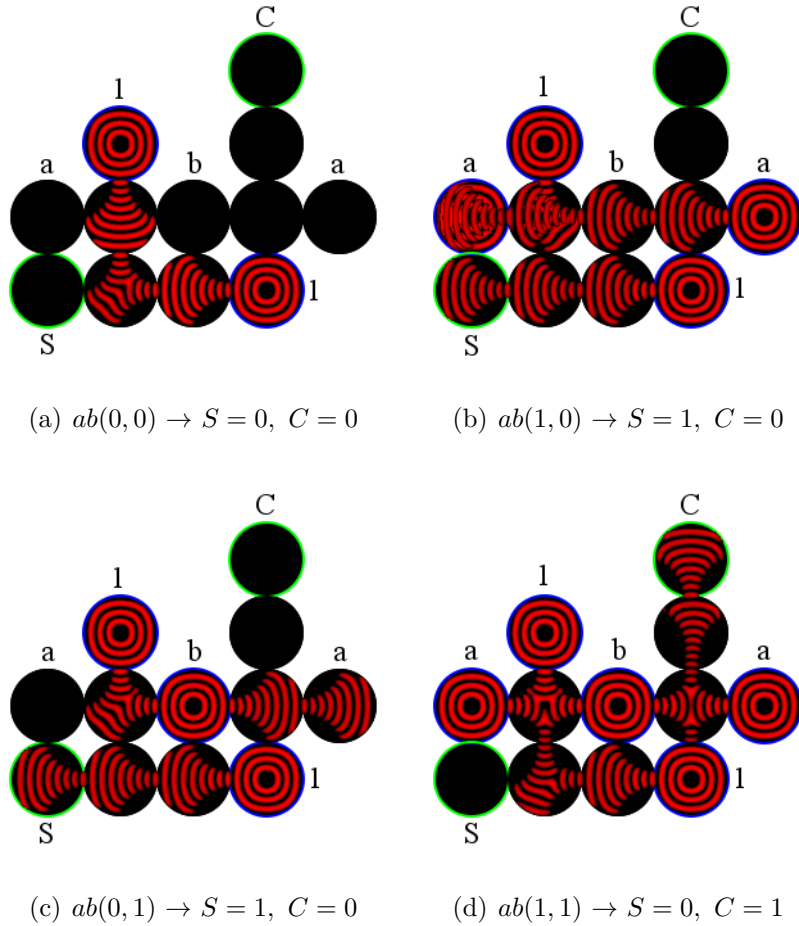


Figure 14: Half adder circuit ($S = a \oplus b$, $C = a \bullet b$) where inputs are located along the central row, a far left, b central and then a repeated far right (blue rings), two source inputs located top left and bottom right (blue ring). The output cell is bottom left (green ring). The circuit is constructed by combining an XOR gate (Fig. 12) (bottom left) and the AND gate (Fig. 8) (top right). The issue of the signal passing problem is obviated by replicating one of the inputs ' a ' (see *signal passing problem* below).

path allowing a' to cross b . A time shift t_d now exists between a, b and a', b so any further processing between a' and b must therefore delay b by t_d . This strategy relies on allowing sufficient time for the refractory tail of signal b to have a negligible effect on a . If the signals are not sufficiently separated then b will extinguish a' which can in another context be used as another logical

construction (Fig. 16).

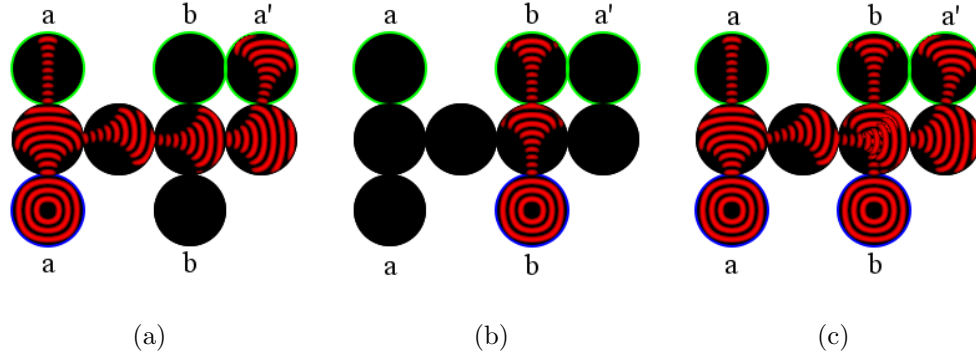


Figure 15: Signal passing problem resolved by sharing the same space (a *cross road*) but at different times. Signals travel from bottom to top. (a) Shows the independent path of signal a . The signal is split by using a broad band aperture at the junction between the 1^{st} and 2^{nd} disc to create a' . (b) Shows the independent path of signal b . (c) Shows a' crossing b .

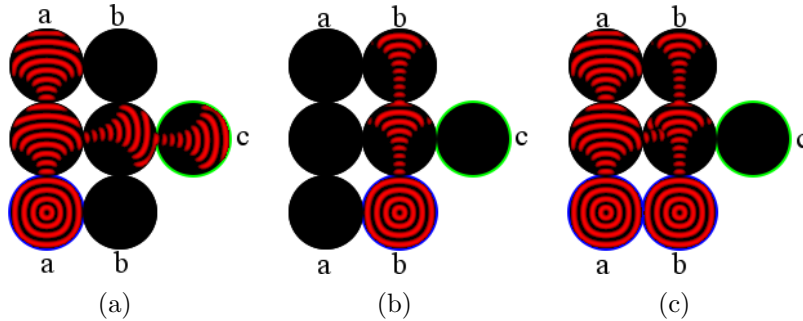


Figure 16: Signal passing gate. When the time difference between two signals trying to cross is too small the refractory tail of one signal will cause extinction in the other. This feature can be exploited to create another logic gate. The output in this gate produces $c = a \bullet \bar{b}$. (a) Shows the independent path of signal a . Signal a is split by using a broad band aperture at the junction between the 1^{st} and 2^{nd} disc to create a' . (b) Shows the independent path of signal b . (c) The refractory tail of b extinguishes signal a' .

Venturing into 3 dimensions (3D) resolves the signal passing problem all together, allowing signals to be routed vertically. At this stage only 2 dimensional (2D) structures of discs have been explored, but these are approximations of our target computation node, a 3D BZ vesicle. In this current

2D perspective, overcoming the signal passing problem via interconnecting linking layers above and below planular 2D functions seems the next logical step analogous to a methodology used in 2 layer and multilayer electronic circuit boards.

Another specific solution for the half adder circuit which removes the need to repeat one of the inputs is possible if all the signal modulation techniques are exploited; disc connection geometry, disc size and aperture efficacy (Sect. 2.2). Figure 17 demonstrates a half adder design where most of the processing occurs in one central reactor disc. The central disc achieves the AND function (Fig. 17c) and the XOR function (Fig. 17b & c). Considering the central disc principally in terms of an AND gate; then the XOR function can be considered as being derived from the AND gate response to input sets $(a, b)(0, 1)$ and $(a, b)(1, 0)$. The outputs of which are curved around into an OR gate in the S output disc creating the XOR function.

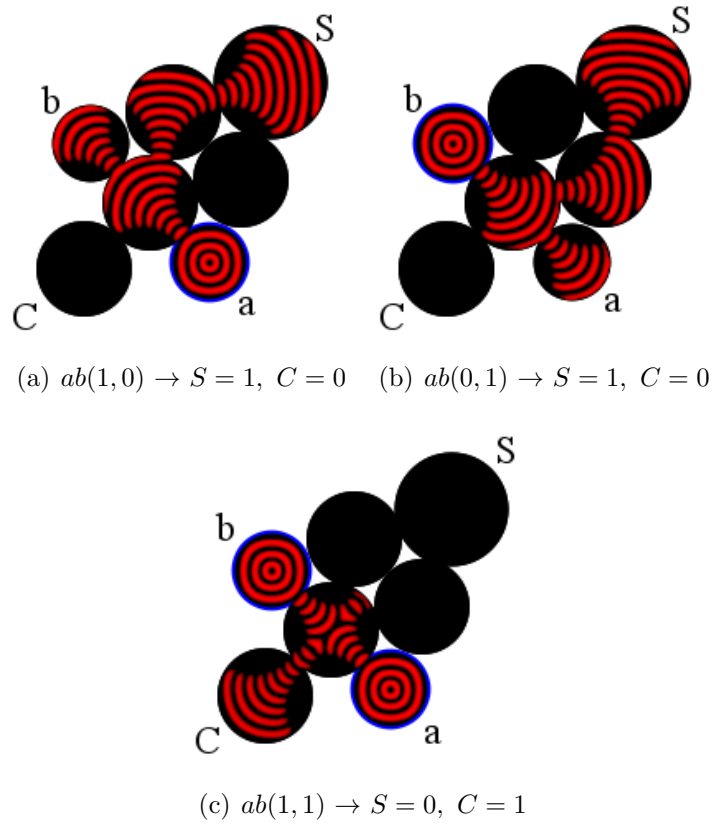


Figure 17: Composite half adder circuit ($S = a \oplus b$, $C = a \bullet b$) where inputs and outputs are all connected to a central reactor disc which can achieve both the AND and XOR function. The two *half* outputs from the XOR operation are recombined with an OR operation with addition discs in the top right. The circuit uses all 3 methods of modulation, connection angle, disc size and aperture efficacy (Sect. 2.2).

3.3. Memory cells

Memory is an essential facet of both adaptive behaviour in Nature and in synthetic computation. It permits animals and machines to build an internal state independent from the current external world state. In this section we present a simple 1 bit volatile read write memory cell constructed entirely with BZ discs. The cell design is independent but similar to previous designs [26, 27] in so much that the existence or absence of a rotating wave represents the setting or resetting of 1 bit of information.

When two BZ waves progress in opposite directions around an enclosed channel, loop or ring of connected discs, then at some point the two opposing wave fronts will meet and are always mutually annihilated (Fig. 19a). Nevertheless, if a unidirectional wave can be inserted into the loop then that wave front will rotate around the loop indefinitely⁷ (Fig. 19b). Furthermore the rotating wave can be terminated by the injection of another asynchronous wave rotating in the opposite direction (Fig. 19.c). Opposing inputs into a loop are analogous to a memory *set* or *reset*. Reading the state of the cell without changing the state can be achieved by connecting another output node where a stream of pulses can be directed to modulate other circuits [20].

The loop and a unidirectional gate (diode) are the two key constructions of this type of memory cell. Unidirectional gates in BZ media have previously been created by exploiting asymmetric geometries or chemistry on either side of a barrier [10]. An alternative design is possible however using discs connected with different apertures. Figure 18 illustrates a diode constructed from a right angle junction connected by a broad band (type J2) aperture to a vertical column and by a narrow beam (type J1) aperture to a horizontal row. Signal flow is only possible from bottom to top ($a \rightarrow b$) because of the asymmetric apertures in the right angle connecting the disc. The operation relies on the relationship between the wave expansion and the angle of the connection. Fine control of the wave beam would in theory allow other angles of connectivity [5] and other functions. In practice fine control of wave diffusion is however difficult to achieve and hence we have restricted our choice between just two types.

As the rotating wave progresses around the loop in the memory cell illustrated in Fig. 19, the opposing input cell also inadvertently becomes an output cell. This may be undesirable in some designs but can be easily re-

⁷For as long as the chemical reagents can sustain the reaction.

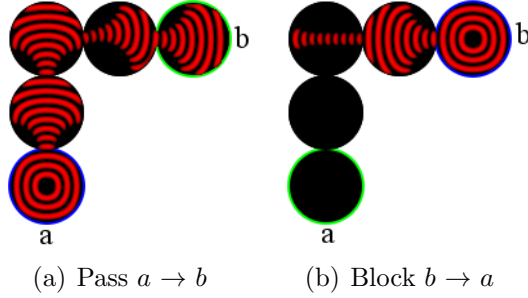


Figure 18: BZ disc diode. (a) Signal propagates from bottom to top ($a \rightarrow b$). A broad band (type J2) aperture at the 2nd (right angle) junction connection permits the signal to expand horizontally towards b . (b) Signal propagates from right to left ($b \rightarrow a$). Conversely the narrow band junction at the 2nd (right angle) junction prohibits propagation towards a .

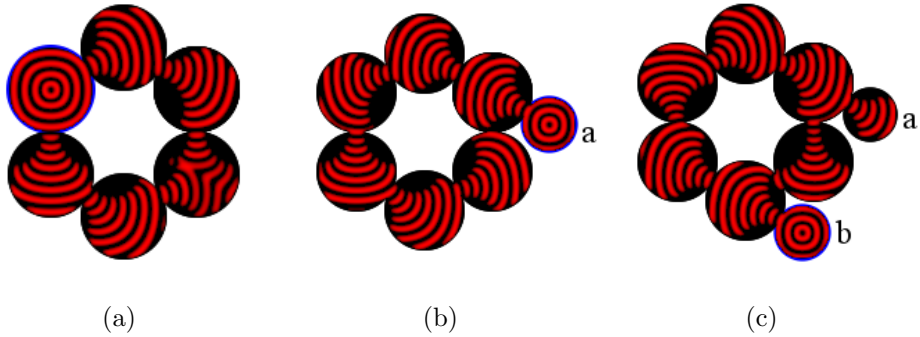


Figure 19: Memory cell development. (a) Hexagonal connected loop of discs, perturbing the medium in any of the cells always leads to complete wave extinction as counter-clockwise and clockwise wave fronts meet at some point during the path. (b) Insertion of a angled *diode* junction inserts a uni-direction (counter-clockwise) wave that rotates indefinitely (in simulation). (c) Addition of another opposing diode junction provides for the insertion of uni-directional (clockwise) wave. Insertion of a wave from either input disc (a — b) can be cancelled by inserting another asynchronous uni-directional wave from the other opposing disc. Inserting more than one wave is not sustainable and always results in a reduction to one wave front.

solved by adding another pair of diode junctions to the circuit. Figure 20 shows such a design, where opposing inputs are not affected by the opposing input.

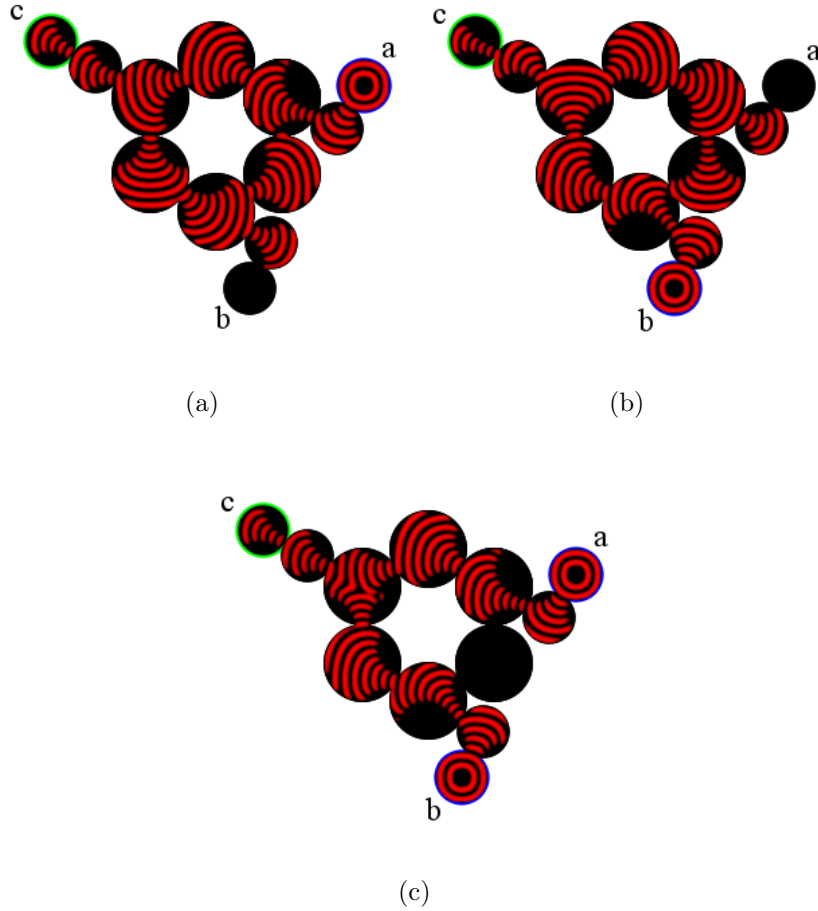


Figure 20: Memory cell with additional diodes on the cell inputs. Two additional angled diode junctions are added to each of the input discs (a & b). This prevents a reverse wave flow back down either of the inputs. An example output disc is also connected (top left). (a) Wave insertion at (top right) a input node results in a persistent counter-clockwise wave. Reverse wave flow down the opposing (bottom) input is blocked by an angled diode junction. (b) Wave insertion at (bottom) b input node results in a persistent clockwise wave. Reverse wave flow down the opposing (top right) a input is likewise, blocked by an angled diode junction. (c) Simultaneous a & b inputs produce one output pulse (c) and annihilate wave rotation.

4. Discussion

Our research is an exploratory component within a collaborative project that aims to create a lipid encapsulated BZ vesicle and organise those vesicles into a functional network. The lipid membrane and the non-linear oscillatory nature of the BZ medium encodes some of the features apparent in biological information processing. Whilst inter-neuron communication is electrical, modulation of that activity is chemical and in the case of individual neurons modulation dominates at the synaptic junction. The membrane between two vesicles can be considered a simple analog of the synaptic junction, a small contact area that can modulate signals in between vesicles. Similarly the electric upstate firing and downstate quiescence of neural signalling is an analog of chemical excitation and refraction. Connecting vesicles together presents the fascinating possibility of creating a chemical processing device similar in principle to biological systems. [29]

Another analog between Natural processing and vesicles is the relationship to artificial Life. The *cell* is the building block of all known life on Earth. Mechanistic explanation for the genesis of Life and the cell remain elusive, but a key aspect of cell morphology is the concept of a cell wall and the ability to separate one state (the outside) from another (the inside), the possibility for an increase in entropy [21]. One theory (amongst many) is a role for lipids in the spontaneous formation of simple cells and hence the development of a separate entity different from the surrounding environment. Whether spontaneous lipid cell formation played a role in early Life remains to be seen, but the principle of an enclosing membrane to a cell like unit appears essential in order separate environment from agent. Enclosing a nonlinear chemical oscillator such as the BZ reaction into a cell (vesicle) leads to another type of phenomena. If the reaction (upstate) in a vesicle can in some degree migrate across the membrane then the reaction in one vesicle could influence the reaction in another, and in turn be subject of influence. The nature of the excited and refractory temporal dynamics of the reaction can lead to interesting emergent ensemble behaviour [40]. Computer simulations of such behaviour of similar simple processing units, known as ‘*Cellular Automata*’ (CA) has been extensively studied [42] and can lead to interesting Life like behaviour [12].

The exploration in the computation modalities of BZ encapsulated vesicles is promising then on (at least) two levels. The macro scale of organised behaviour (classification of this work) and the small scale emergent oscil-

latory behaviour analogous to cellular automata. The parallel between the notion of a conscious single thread behaviour and the unconscious parallel emergent behaviour. In this study we have shown that most of the computation accomplishments of previous geometrically constrained BZ processing at the macro scale can be achieved with BZ discs alone. In extrapolating discs into spherical vesicles more interesting behaviour and processing is likely to be possible⁸ albeit at the cost of the simplicity and clarity of design.

5. Future work

Experiments are currently in progress to replicate these simulation results in real chemistry (an example of the AND gate is shown in the appendix (Sect. 7)). Our goal is to explore computational modalities of interconnected discs and vesicles. In doing so we hope that such work will both inspire novel chemical computing and introduce new strategies for use in existing systems and other mediums (including silicon) or conventional computers. Implementing devices that are known to be an essential to perform conventional computation is useful for demonstrative purposes. Expunging the computing capabilities of geometrically modulated reaction diffusion computers. Nevertheless the innate massively parallel and deep temporal-spatial nature of such a substrate is a good candidate to explore the kind of computation problems for which vonn Neumann architecture machines perform so poorly. Previous studies have shown that RD systems are capable of performing computation in the conventional paradigm and this study has shown that distributing encapsulated RD units in cell like units is equally competent. On that basis other perhaps unknown structures and strategies could be developed beyond our current understanding. To achieve these aims and in part, not to be biased by known solutions and tradition design methodology our next step is to apply an evolutionary strategy to evolve functional networks of discs. We intend to focus on solving computational tasks for which the solutions are currently protracted in conventional systems.

6. Summary

Creating components, gates and circuits commonly used in the design of discrete conventional computers within geometrically constrained construc-

⁸The innate resolution of the signal passing problem (Sect.3.2) for example.

tions containing sub-excitable BZ media has been extensively studied both in simulation and real chemistry. This work has shown that some of the previous circuits, logic gates, composite logic gate circuits (the half adder) and memory can be reproduced using networks of interconnected discs alone. Wave modulation through discs can be manipulated by changing the network interconnections, relative disc sizes and aperture efficiency. All the designs presented rely on a uniform excitability level of the reaction. This is an important consideration since discs or vesicles whose function relies on non-uniform excitation levels may eventually fail as reagents equalise across connecting junctions, additionally photo modulation of excitability is possible with discs in 2 dimensions, but otherwise impossible with vesicles in 3 dimensional structures. Elementary and universal logic gates and composite circuits have also been shown possible with a uniform disc size and aperture gap connected in a simple orthogonal network structure, whereas other circuits such as the diode and memory cell rely on a combination of different geometric connectivity, disc size and aperture efficacy.

7. Appendix

An example of some initial results from on-going laboratory work is shown in Fig. 21a. An identical background image generated from the simulation software, where light intensity is proportional to ϕ and is projected onto a thin layer of silica gel containing a photo sensitive $(\text{Ru}(\text{bpy})_3^{2+})$ catalyst for the BZ reaction. The gel is submerged in catalyst-free BZ reagents (NaBrO_3 , $\text{CH}_2(\text{COOH})_2$, H_2SO_4 & BrMA).⁹ Waves are continuously initiated by inserting silver colloidal particles onto the gel surface at the center of the two input discs (dark centers, top left and right). Fine waves can be seen travelling out from each input disc, colliding in the central disc and then expanding into the output disk (bottom). For comparison the result of the simulated AND gate (Sect. 3.1) is shown in the adjacent frame (Fig. 21b). The real chemistry image (Fig. 21a) is a single image of multiple wave initiations, whereas the simulation image (Fig. 21b) is a composite of time lapse images of a single wave initiation.

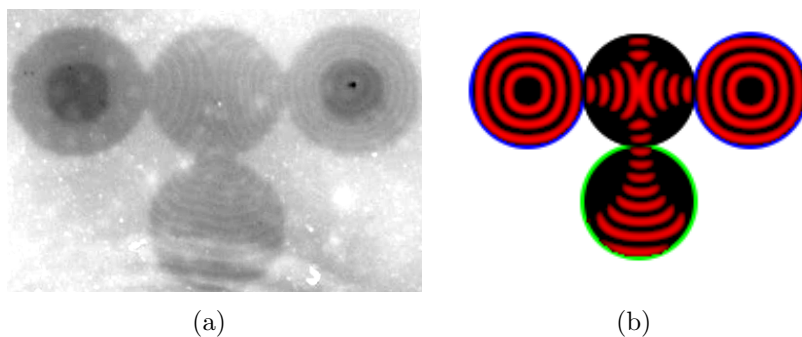


Figure 21: Example of laboratory work in progress. (a) AND gate response to $(a, b)(1, 1) \rightarrow 1$ in real chemistry experiment. Fine wave fragments can be observed travelling from the input zones (dark areas, top left and right) and moving into the output disk as a result of collisions in the central disc. Disc diameter $\sim 14\text{mm}$, time duration from initiation to output cell bottom wall was $\sim 510\text{s}$. (b) AND gate simulation $(a, b)(1, 1) \rightarrow 1$ repeated for comparison from Sect. 3.1. Input discs are top left and right (blue rings), the output disc is bottom central (green ring).

⁹Further details of chemistry and experimental apparatus are described in [39].

8. Acknowledgements

The work is part of the European project 248992 funded under 7th FWP (Seventh Framework Programme) FET Proactive 3: Bio-Chemistry-Based Information Technology CHEM-IT (ICT-2009.8.3). The authors wish to acknowledge the support of the EPSRC grant number EP/E016839/1 for support of Ishrat Jahan. We would like to thank the project coordinator Peter Dittrich and project partners Jerzy Gorecki and Klaus-Peter Zauner for their inspirations and useful discussions [29].

References

- [1] Adamatzky, A., 2009. From reaction-diffusion to physarum computing. *Natural Computing* 8 (3), 431–447.
- [2] Adamatzky, A., Arena, P., Basile, A., Carmona-Galan, R., Costello, B., Fortuna, L. Frasca, M., Rodriguez-Vazquez, A., May 2004. Reaction-diffusion navigation robot control: From chemical to VLSI analogic processors. *IEEE Transactions on Circuits and Systems I: Regular Papers* 51 (5), 926–938.
- [3] Adamatzky, A., De Lacy Costello, B., October 2002. Collision-free path planning in the Belousov-Zhabotinsky medium assisted by a cellular automaton. *Naturwissenschaften* 89 (10).
- [4] Adamatzky, A., De Lacy Costello, B., Asai, T., 2005. *Reaction-Diffusion Computers*. Elsevier Science Inc., New York, NY, USA.
- [5] Adamatzky, A., De Lacy Costello, B., Bull, L., June 2010. On polymorphic logical gates in sub-excitable chemical medium. <http://arxiv.org/abs/1007.0034>.
- [6] Adamatzky, A., De Lacy Costello, B., Bull, L., Stepney, S., Teuscher, C. (Eds.), 2006. *Unconventional Computing 2007*. Luniver Press.
- [7] Adamatzky, A., De Lacy Costello, B., Melhuish, C., Ratcliffe, N., 2004. Experimental implementation of mobile robot taxis with onboard Belousov-Zhabotinsky chemical medium. *Materials Science and Engineering: C* 24 (4), 541 – 548.

- [8] Adamatzky, A., De Lacy Costello, B., Ratcliffe, N. M., 2002. Experimental reaction-diffusion pre-processor for shape recognition. *Physics Letters A* 297 (5-6), 344 – 352.
- [9] Adamatzky, A., Holley, J., Bull, L., De Lacy Costello, B., June 2010. On computing in fine-grained compartmentalised Belousov-Zhabotinsky medium. <http://arxiv.org/abs/1006.1900>.
- [10] Agladze, K., Aliev, R. R., Yamaguchi, T., Yoshikawa, K., 1996. Chemical diode. *Journal of Physical Chemistry* 100 (33), 13895–13897.
- [11] Agladze, K., Magome, N., Aliev, R., Yamaguchi, T., Yoshikawa, K., 1997. Finding the optimal path with the aid of chemical wave. *Physica D: Nonlinear Phenomena* 106 (3-4), 247 – 254.
- [12] Berlekamp, E. R., Conway, J. H., Guy, R. L., 1982. *Winning Ways for your Mathematical Plays*. Vol. 2. Academic Press.
- [13] Bollt, E. M., Dolnik, M., Jun 1997. Encoding information in chemical chaos by controlling symbolic dynamics. *Phys. Rev. E* 55 (6), 6404–6413.
- [14] Fredkin, E., Toffoli, T., 2002. Conservative logic, 47–81.
- [15] Gorecka, J., Gorecki, J., Igarashi, Y., Feb 2007. One dimensional chemical signal diode constructed with two nonexcitable barriers. *The Journal of Physical Chemistry* 111 (5), 885–889.
- [16] Gorecki, J., Gorecka, J., 2005. Chemical programming in reaction-diffusion systems. In: Adamatzky, A., Teuscher, C. (Eds.), *Unconventional Computing 2005: From Cellular Automata to Wetware*. Luniver Press, pp. 1–12.
- [17] Gorecki, J., Gorecka, J. N., 2005. On mathematical description of information processing in chemical systems. In: T., A., Niezgodka, M. (Eds.), *Mathematical approach to nonlinear phenomena; Modeling, analysis and simulations*. Vol. 23 of GAKUTO International Series, *Mathematical Sciences and Applications*. pp. 73–90.
- [18] Gorecki, J., Gorecka, J. N., 2009. Computing in geometrical constrained excitable chemical systems. In: Meyers, R. A. (Ed.), *Encyclopedia of Complexity and Systems Science*. Springer-Verlag.

- [19] Gorecki, J., Gorecka, J. N., Igarashi, Y., 2009. Information processing with structured excitable medium. *Natural Computing: an international journal* 8 (3), 473–492.
- [20] Gorecki, J., Yoshikawa, K., Igarashi, Y., 2003. On chemical reactors that can count. *Journal of Physical Chemistry* 107 (10), 1664–1669.
- [21] Harold, F., 2001. *The Way of the Cell*. Oxford University Press, New York.
- [22] Igarashia, Y., Jerzy Greckia, b., Greckac, J. N., 2008. One dimensional signal diodes constructed with excitable chemical system. *Acta Physica Polonica B* 39 (5), 1187–1197.
- [23] Kuhnert, L., 1986. A new optical photochemical memory device in a light-sensitive chemical active medium. *Nature* 319, 393–394.
- [24] Kuhnert, L., Agladze, K. I., , Krinsky, V. I., January 1989. Image processing using light-sensitive chemical waves. *Nature* 337, 244–247.
- [25] Kusumi, T., Yamaguchi, T., Aliev, R. R., Amemiya, T., Ohmori, T., Hashimoto, H., Yoshikawa, K., 1997. Numerical study on time delay for chemical wave transmission via an inactive gap. *Chemical Physics Letters* 271 (4-6), 355–360.
- [26] Motoike, I., Yoshikawa, K., May 1999. Information operations with an excitable field. *Phys. Rev. E* 59 (5), 5354–5360.
- [27] Motoike, I. N., Yoshikawa, K., Iguchi, Y., Nakata, S., Feb 2001. Real-time memory on an excitable field. *Phys. Rev. E* 63 (3), 036220.
- [28] Nagahara, H., Ichino, T., Yoshikawa, K., 2008. Direction detector on an excitable field: Field computation with coincidence detection. <http://arxiv.org/pdf/nlin/0405063>.
- [29] NeuNeu, 2010. NeuNeu: Artificial wet neuronal networks from compartmentalised excitable chemical media project. <http://neu-n.eu/>.
- [30] Noyes, R. M., Field, R., Koros, E., Feb 1972. Oscillations in chemical systems. i. detailed mechanism in a system showing temporal oscillations. *Journal of the American Chemical Society* 94 (4), 1394–1395.

- [31] Press, W. H., Flannery, B. P., Teukolsky, S. A., Vetterling, W. T., Oct 1992. Numerical Recipes in C: The Art of Scientific Computing, 2nd Edition. Cambridge University Press, England.
- [32] Rambidi, N. G., Yakovenchuk, D., 1999. Finding paths in a labyrinth based on reaction-diffusion media. *Biosystems* 51 (2), 67 – 72.
- [33] Rambidi, N. G., Yakovenchuk, D., Jan 2001. Chemical reaction-diffusion implementation of finding the shortest paths in a labyrinth. *Phys. Rev. E* 63 (2), 026607.
- [34] Stanley, C. E., Elvira, K. S., Niu, X. Z., Gee, A. D., Ces, O., Edel, J. B., deMello, A. J., 2010. A microfluidic approach for high-throughput droplet interface bilayer (dib) formation. *Chem. Commun.* 46, 1620–1622.
- [35] Steinbock, O., Kettunen, P., Showalter, K., 1996. Chemical wave logic gates. *Journal of Chemistry Physics* 100, 18970–18975.
- [36] Steinbock, O., Toth, A., Showalter, K., 1995. Navigating complex labyrinths: Optimal paths from chemical waves. *Science* 267 (5199), 868–871.
- [37] Szymanska, J., Igarashia, Y., Goreckia, J., Gorecka, J. N., 2010. Belousov-Zhabotinsky reaction in lipid covered droplets. (In press).
- [38] Toth, A., K.Showalter, 1995. Logic gates in excitable media. *Journal of Chemistry Physics* 103, 2058–2066.
- [39] Toth, R., Stone, C., Adamatzky, A., De Lacy Costello, B., Bull, L., 2009. Experimental validation of binary collisions between wave fragments in the photosensitive Belousov-Zhabotinsky reaction. *Chaos, Solitons & Fractals* 41 (4), 1605 – 1615.
- [40] Vanag, V. K., Epstein, I. R., Nov 2001. Pattern formation in a tunable medium: The Belousov-Zhabotinsky reaction in an aerosol OT microemulsion. *Phys. Rev. Lett.* 87 (22), 228301.
- [41] von Neumann, J., 2005. John von Neumann: Selected Letters. American Mathematical Society, London.

- [42] Wolfram, S., 2002. *A New Kind of Science*. Wolfram Media.
- [43] Zaikin, A. N., Zhabotinsky, A. M., 1970. Concentration wave propagation in two-dimensional liquid-phase self-oscillating system. *Nature* 225 (5232), 535–537.
- [44] Zhabotinsky, A. M., Zaikin, A. N., 1973. Autowave processes in a distributed chemical system. *Journal of Theoretical Biology* 40 (1), 45 – 61.